

MODELLING AND PREPARATION OF CORE FOAMED Al PANELS WITH ACCUMULATIVE HOT-ROLL BONDED PRECURSORS

NAČRTOVANJE IN IZDELAVA Al-PANELOV S SREDICO IZ Al-PEN NA OSNOVI VEČSTOPENJSKO TOPLO VALJANIH PREKURZORJEV

**Varužan Kevorkijan¹, Uroš Kovačec², Irena Paulin³, Srečo Davor Škapin⁴,
Monika Jenko³**

¹Independent Researcher, Betnavska cesta 6, 200 Maribor, Slovenia

²Impol Aluminium Industry, Partizanska 38, 2310 Slovenska Bistrica, Slovenia

³Institute of Metals and Technology, Lepi pot 11, 1000 Ljubljana, Slovenia

⁴Institut "Jožef Stefan", Jamova 39, 1000 Ljubljana, Slovenia
varuzan.kevorkijan@impol.si

Prejem rokopisa – received: 2011-08-29; sprejem za objavo – accepted for publication: 2011-10-25

In this paper, laboratory and semi-industrial processes for the preparation of aluminium foam samples and core-foamed panels with closed porosity were investigated. The samples were prepared starting from the accumulative hot-roll bonded precursors, with titanium hydride (TiH_2) or dolomite ($\text{Ca}_{0.5}\text{Mg}_{0.5}\text{CO}_3$) powder added as the foaming agent. The formation of the precursors was performed in three steps. In the initial stage, titanium dihydride or dolomite particles were deposited on a single side of a selected number of aluminium strip samples made from the alloy AA 1050. In the second step, by putting together in pairs, single-sided coated strips, precursors with a two-layered structure were prepared. The samples were hot-rolled to a final thickness of 1.9–3.8 mm, introducing a total deformation of about 45–49 % by a process well-known as accumulative hot-roll bonding. In the third stage of the precursor's formation, the desired multilayered precursor's structure was achieved by hot-roll multi-passing, i.e., by repeating (with 2–16 passes) the accumulative hot-roll bonding procedure. The obtained precursors were foamed in an electrical furnace, under different foaming conditions, based on the initial temperature of the thermal decomposition of the foaming agent. The microstructure of the obtained foam samples was investigated with optical and scanning electron microscopy. According to the accumulated experimental results, one can conclude that the usage of dolomite powder as a foaming agent with a higher temperature of thermal decomposition ($>750\text{ }^\circ\text{C}$) compared to TiH_2 , which thermally decomposed even at the temperature of hot-rolling ($>350\text{ }^\circ\text{C}$), enabling the formation of multilayered precursors at higher temperatures of hot-rolling without any intermediate annealing. This consequently increases the productivity of the foamed core panel production without influencing their final quality.

Key words: Al foams, core foamed Al panels, precursors preparation, accumulative hot-roll bonding, comparison of different foaming agents, characterisation

V delu opisujemo razvoj laboratorijskih in polindustrijskih postopkov priprave vzorcev aluminijskih pen in panelov iz Al-pen z zaprtro poroznostjo. Vzorce panelov smo izdelovali na osnovi večstopenjsko toplo valjanih prekurzorjev, ki so kot sredstvo za penjenje vsebovali delce titanovega dihidrida (TiH_2) ali dolomitnega prahu ($\text{Ca}_{0.5}\text{Mg}_{0.5}\text{CO}_3$). Postopek priprave večplastnih prekurzorjev je potekal v treh fazah. V začetni fazi smo delce titanovega dihidrida ali dolomita nanašali na izbrano stran aluminijevega traku zlitine AA 1050. Sledila je priprava

dvoplastnega prekurzorja. Po dva in dva premazana trakova smo zložili tako, da sta se premazani stranici stikali ter dvojček vroče zvaljali na 1,9–3,8 mm s skupno deformacijo med 45–49 %. Postopek smo v sklepni fazi izdelave prekurzorjev ponavljali do želene večplastnosti (od 2- do 16-krat). S postopkom večkratnega valjanja in podvajanja plasti penilnega sredstva smo dosegli enakomerno porazdelitev penilnega sredstva skozi celoten prerez izdelanih prekurzorjev. Dobljene prekurzorje smo nato penili v električni peči pri različnih pogojih glede na temperaturo termičnega razkroja sredstva za penjenje. Mikrostrukturo dobljenih vzorcev pen smo analizirali z optično in vrstično elektronsko mikroskopijo. Z raziskavami smo potrdili, da uporaba dolomitnega prahu kot penilnega sredstva z višjo temperaturo termičnega razkroja ($>750\text{ }^\circ\text{C}$) v primerjavi s TiH_2 , ki se termično razkroja že pri temperaturi toplega valjanja ($>350\text{ }^\circ\text{C}$), omogoča izdelavo večplastnih prekurzorjev pri višjih temperaturah toplega valjanja brez vmesnega žarjenja in posledično povišuje produktivnosti brez vpliva na kakovost končnega izdelka.

Ključne besede: Al-pene, Al-paneli s penasto sredico, priprava prekurzorjev, večstopenjsko toplo valjanje, primerjava različnih sredstev za penjenje, karakterizacija

1 INTRODUCTION

Accumulative Roll Bonding (ARB) is a new and promising manufacturing process for closed-cell aluminium foams and core-foamed panels¹⁻³. The ARB process, as one of the severe plastic deformation processes, has been applied to many metals and alloys to produce an ultra-fine crystal grains structure. The processing procedure is presented in **Figure 1**.

Instead of aluminium powder, Al sheet is applied as a starting material, making this processing route cost-effective and promising for further industrialization. During the first stage, two aluminium strips are stacked with the appropriate amount of selected blowing-agent powder of the proper morphology. Second, the strip is roll-bonded by a 50 % reduction and cut into two. After repeatedly covering the surface with blowing agent, the two strips are stacked to be the initial dimension, and then roll-bonded again. Since these procedures can be repeated indefinitely, the desired multilayered precursor's structure could be achieved. By multiplying the foaming-agent layers, its uniform distribution across the entire cross-section of the prepared precursor can be achieved. Finally, the obtained precursors are foamed to the end products: foamed aluminium sheet or core-foamed panels.

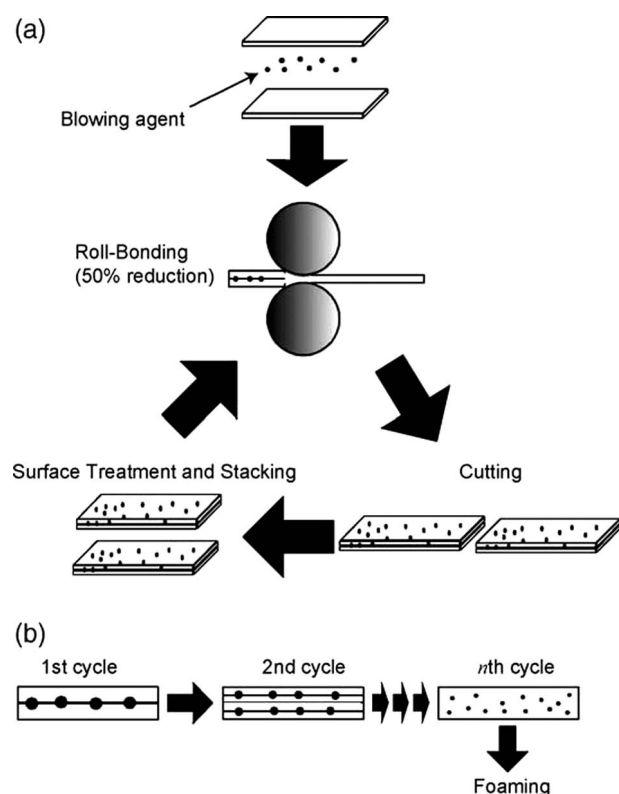


Figure 1: (a) Schematic illustration of the manufacturing process of a precursor sheet using the ARB process. (b) Prediction of gradual distribution of added foaming-agent particles³.

Slika 1: (a) Shematski prikaz postopka večstopenjskega topllega valjanja prekurzorja; (b) prikaz porazdelitve delcev penila v večplastnem prekurzorju³.

Investigations performed in the past few years have confirmed the great potential of the ARB processing route in the cost-effective and highly productive fabrication of foamed aluminium sheets and various core-foamed panels by TiH₂ as a foaming agent^{3,4}. An additional reduction in cost can be achieved by replacing the expensive TiH₂ with alternative, inexpensive foaming agents, particularly carbonates, among which natural carbonates such as CaCO₃ marble powder or CaMg(CO₃)₂ dolomite powder are particularly attractive.

Successfully replacing the TiH₂ with carbonates in the foaming precursor fabricated by the powder metallurgical or stir-casting route has been reported by several authors⁵⁻⁹. However, similar investigations of replacing the TiH₂ foaming agent with dolomite particles in accumulative hot-roll bonded precursors are still not completed. Therefore, the purpose of this work was to investigate the possible benefits of replacing TiH₂ with dolomite particles in multilayered precursors made by ARB.

2 EXPERIMENTAL PROCEDURE

The samples were prepared by starting from the accumulative hot-roll bonded precursors, with titanium hydride (TiH₂) or dolomite (Ca_{0,5}Mg_{0,5}CO₃) powder added as the foaming agent.

The formation of the precursors was performed in three steps. In the initial stage, titanium dihydride or dolomite particles were deposited on a single side of a selected number of aluminium strip samples (100 mm in width, 200 mm in height and with a thickness of approx. 2–4 mm) made from the alloy EN AW 1050. The suspension of the powdered foaming agent (TiH₂ or MgAl₂O₄) in acetone was spread out on the strip with a painter's roll. Titanium hydride (supplier: AG Materials Inc.) and dolomite powders (supplier: Granit, d. o. o., Slovenska Bistrica, Slovenia) of five different average particle sizes were applied as foaming agents. The average particle size of the powders used in the experiments is listed in **Table 1**. The particle size distribution of the powdered foaming agents was measured using laser particle analyzer (Malvern Mastersizer 2000). The relative error of the measurement was within ±1 %.

The surface concentration of the foaming agent achieved after removing the acetone was between approximately 2.5×10^{-3} and 3.75×10^{-3} mg/mm². In the second step, by putting together in pairs single-sided coated strips, precursors with a two-layered structure were prepared. The samples were hot-rolled to a final thickness of 1.9–3.8 mm, introducing a total deformation of about 45–49 % by a process that is well known as accumulative hot-roll bonding. It was found that the consistency of the obtained precursors (the adhesion between two layers) was strongly affected by the parameters of the hot-rolling (the strip deformation and the temperature of the hot-rolling). These were signifi-

Table 1: The average particle size and the cumulative particle size distribution of the TiH_2 and dolomite powder applied as foaming agents

Tabela 1: Povprečna velikost delcev in porazdelitev delcev po velikosti TiH_2 in dolomitnega prahu, uporabljenih kot sredstvo za penjenje

TiH ₂ powder	TIH-0420
Average particle size (μm)	20.4
Cumulative particle size distribution (μm)	
<i>D</i> ₁₀	13.1
<i>D</i> ₂₅	17.4
<i>D</i> ₅₀	20.4
<i>D</i> ₇₅	23.7
<i>D</i> ₉₀	41.4
Uniformity of particle size distribution (μm)	
<i>D</i> ₉₀ – <i>D</i> ₁₀	28.3
Dolomite powder	D-4
Average particle size (μm)	20.8
Particle size distribution	
<i>D</i> ₁₀	11.2
<i>D</i> ₂₅	15.9
<i>D</i> ₅₀	20.8
<i>D</i> ₇₅	23.1
<i>D</i> ₉₀	27.2
Uniformity of particle size distribution (μm)	
<i>D</i> ₉₀ – <i>D</i> ₁₀	16.0

cantly limited by the technical possibilities of the existing mini hot-rolling mill. The diameter of the working rolls was only 200–450 mm. However, by carefully selecting the optimal power of the hot-rolling mill unit (about 18–50 kW) for the proper deformation of the strip and the temperature of the hot-rolling (between 300–350 °C), the complete recrystallization of the strip was achieved, avoiding in that way any possible hardening of the wrought aluminium alloy. In the third stage of the precursor's formation, the desired multilayered precursor's structure was achieved by hot-roll multi-passing, i.e., by repeating (with 2–16 passes) the accumulative hot-roll bonding procedure. By the multiple accumulative hot-roll bonding and by doubling the layers of the foaming agent, its uniform distribution was achieved across the entire cross-section of the prepared precursors.

The precursors were foamed in a conventional batch electrical furnace with air-atmosphere circulation under various experimental conditions (time, temperature) and by applying the same cooling method. Before foaming, the individual precursors were placed on a ceramic plate covered by a boron nitride layer. The plate dimensions and the precursor size 100 mm × 100 mm were selected to allow the complete expansion of the precursor to foam. The arrangement was placed inside a pre-heated batch furnace at a selected temperature and held for the selected holding time. In samples with TiH_2 , thermal decomposition was observed, starting from approximately

350 °C. These samples were foamed at 700–750 °C, for 3–18 s. Samples with the dolomite foaming agent, for which the thermal decomposition is initiated above 750 °C, were foamed at 780 °C for 2–5 min. After that, the sample was removed from the furnace and the foaming process was stopped by rapid cooling with pressurised air to room temperature. The thermal history of the foam sample was recorded, using a thermocouple located directly in the precursor material. The density of the foam was calculated using Archimedes' method. The porosity of the manufactured foam was calculated using the rate: 1-(foam density/aluminium density). Macro and microstructural examinations were performed on sections obtained by wire precision cutting across the samples and on samples mounted in epoxy resin, using optical and scanning electron microscopy (SEM/EDS). The average particle size of the pores in the foams was estimated by analysing optical and scanning electron micrographs of the as-polished foam bars using the point-counting method and image analysis and processing software.

3 MODELLING OF THE SURFACE CONCENTRATION AND MORPHOLOGY OF THE FOAMING AGENT IN ARB PRECURSORS

In precursors fabricated by the ARB processing route, the proper surface concentration and morphology of the foaming agent are crucial for the development of high-quality foams with closed cells and a uniform microstructure. Because of that, it was very important to correlate by the model developed in this work the surface concentration and morphology of the foaming agent with an average cell size and microstructure of the foam.

The particles of foaming agent are, as much as possible, homogeneously dispersed on the surface of the aluminium sheet, as is evident in **Figure 2**.

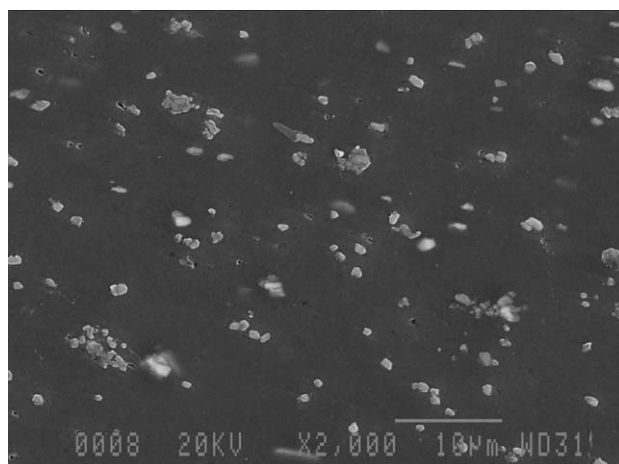


Figure 2: SEM micrograph of the surface of an aluminium sheet after the first cycle of ARB, with homogeneously distributed dolomite particles

Slika 2: SEM-posnetek površine aluminijskega traku po prvem prehodu večstopenjskega toplega valjanja s homogeno porazdeljenimi delci dolomita

The neighbouring particles of foaming agent are mutually apart for an average minimum distance X_{min} . As will be demonstrated in the model, this distance is determined by the surface concentration of the foaming agent C and its average particle size d_{50} .

The surface concentration of the foaming agent is defined as follows:

$$C = m/S \tag{1}$$

Here, m is the total mass of the foaming agent and S is the surface of the aluminium sheet. The molar surface concentration C' is defined as:

$$C' = m/(MS) \tag{2}$$

where M represents the molar mass of the selected foaming agent. Finally, the particle surface concentration C'' is introduced as:

$$C'' = N/S = 1/X_{min}^2 \tag{3}$$

N is the total number of particles of foaming agent:

$$N = m_p/M = d_{50}^3 \pi \rho / 6M \tag{4}$$

In Eq. 4, m_p represents the mass of an average particle of foaming agent, d_{50} is the average particle size and ρ is the theoretical density of the foaming agent.

Therefore, by combining Eqs.1–4 we can derive, for the particle surface concentration, the following expression:

$$C'' = 6C/(d_{50}^3 \pi \rho) \tag{5}$$

and, consequently, for X_{min} :

$$X_{min} = [(d_{50}^3 \pi \rho) / 6C]^{1/2} \tag{6}$$

Applying, for the bubbles' growth, a simple, stoichiometric model, in which the complete thermal decomposition of an individual foaming agent particle provides a gas phase for the bubble's nucleation and growth, the maximum bubble diameter D_{max} can be determined with the ideal gas equation:

$$p_{max} V = nRT \tag{7}$$

where n corresponds to the number of moles of gas phase inside the bubble, V is the bubble volume, R is the universal gas constant and T is the temperature.

p_{max} can be calculated by applying Laplace's equation:

$$p_{max} = (2\sigma_{lg}/r) + \rho gh + p_0 \tag{8}$$

The maximum bubble pressure p_{max} is the sum of the capillary ($2\sigma_{lg}/r$), hydrostatic (ρgh) and atmospheric (p_0) pressures. The capillary pressure depends on the surface tension σ_{lg} at the gas-liquid interface and the bubble radius (r); the hydrostatic pressure is determined by the immersion depth (h) and the density of the molten aluminium alloy (ρ).

By considering a spherical bubble and by combining Eqs. (7) and (8), we can calculate:

$$[(2\sigma_{lg}/r) + \rho gh + p_0] (4/3)r_{max}^3 \pi = nRT \tag{9}$$

During an early stage of the bubble's growth, only the capillary pressure ($2\sigma_{lg}/r$) should be considered, while in the final stage of the bubble's growth the only important pressure is the atmospheric (p_0). Note that for laboratory conditions, the hydrostatic pressure (ρgh) is always negligible.

Based on this, in the case considered by the model:

$$p_{max} = p_0 \tag{10}$$

Therefore, the maximum bubble diameter D_{max} is finally determined by the formula:

$$D_{max} = d_{50} [(kRT\rho)/p_0 M]^{1/3} \tag{11}$$

Here, k represents the stoichiometric constant ($k = 1$ for TiH_2 and $k = 2$ for dolomite), R is the universal gas constant, T is temperature, ρ is the density of the foaming agent, p_0 is the atmospheric pressure and M is the molar mass of the foaming agent. In **Tables 2 and 3**, the calculated values for the maximum bubble radius for cells grown from the TiH_2 and dolomite particles of different initial particle size are listed.

Table 2: Maximum bubble radius for a cell grown from TiH_2 particles with different initial particle sizes (d_{50}).

Tabela 2: Maksimalni premer pore iz TiH_2 delcev različne začetne velikosti (d_{50})

The average particle size of TiH_2 (μm)	3	20	40	75	140
Maximum bubble diameter, D_{max} / μm	54	360	808	1.352	2.526

Table 3: Maximum bubble radius for bubbles created by dolomite particles of different initial particle sizes (d_{50})

Tabela 3: Maksimalni premer pore iz delcev dolomita različne začetne velikosti (d_{50})

The average particle size of dolomite (μm)	3	5	10	20	35
Maximum bubble diameter, D_{max} / μm	40	68	132	268	468

According to the theoretical prediction based on Eq. 11 and the calculated values reported in Tables 2 and 3, at the same initial particle size of the applied foaming agents (3 μm or 20 μm) and the same foaming conditions (temperature, time), the bubbles created by TiH_2 should be coarser.

In order to obtain a stable foam microstructure, with isolated closed cells, it is necessary that:

$$X_{min} > D_{50} \tag{12}$$

By combining Eqs. 6, 11 and 12, the condition (12) leads to the required correlation between the surface concentration and the foaming-agent morphology:

$$C < \text{const.} (d_{50}/T)^{2/3} \tag{13}$$

Based on the model, it is evident that for the selected morphology of the foaming agent d_{50} and foaming temperature T the surface concentration of the foaming agent C cannot be selected arbitrarily, but, in order to achieve a

foam microstructure with stable individual closed cells, it should fulfil the condition expressed by Eq.13.

4 RESULTS AND DISCUSSION

4.1 Foam properties as a function of the composition of accumulative roll-bonded precursors

The results of the investigation of the foam properties (density and cell size distribution) achieved by applying various types (TiH_2 or dolomite) and surface concentrations of foaming agents are reported in **Tables 4 and 5**.

Table 4: The experimentally measured density and cell-size distribution of the aluminium foam samples at various concentrations of TiH_2 foaming agent. The foaming conditions: 700 °C, 120 s.

Tabela 4: Eksperimentalno izmerjene vrednosti gostote in porazdelitve velikosti por v vzorcih aluminjske pene, izdelanih pri različni koncentraciji delcev TiH_2 , uporabljenega kot penila. Pogoji penjenja: 700 °C, 120 s.

Surface concentrations of TiH_2 (mg/mm^2)	2.5×10^{-3}	3.0×10^{-3}	3.5×10^{-3}
Density of Al foam (% T. D.)	25.9 ± 1.3	23.8 ± 1.2	21.2 ± 1.1
Cell size distribution (mm)			
D_{10}	2.6 ± 0.3	3.2 ± 0.3	3.3 ± 0.3
D_{25}	2.7 ± 0.3	3.5 ± 0.3	3.8 ± 0.3
D_{50}	2.8 ± 0.3	3.7 ± 0.4	5.1 ± 0.5
D_{75}	3.0 ± 0.3	4.2 ± 0.3	5.5 ± 0.6
D_{90}	4.6 ± 0.5	8.4 ± 0.3	10.4 ± 1.0
Uniformity of cell size distribution (μm)			
$D_{90}-D_{10}$	2.0 ± 0.2	5.2 ± 0.6	7.1 ± 0.7

Table 5: The experimentally measured density and cell-size distribution of aluminium foam samples at various concentrations of dolomite foaming agent. The foaming conditions: 700 °C, 120 s.

Tabela 5: Eksperimentalno izmerjene vrednosti gostote in porazdelitve velikosti por v vzorcih aluminjske pene, izdelanih pri različni koncentraciji delcev dolomite, uporabljenega kot penila. Pogoji penjenja: 700 °C, 120 s.

Surface concentrations of dolomite (w/%)	2.5×10^{-3}	3.0×10^{-3}	3.5×10^{-3}
Density of Al foam (% T.D.)	15.4 ± 0.8	12.8 ± 0.6	11.1 ± 0.6
Cell size distribution (mm)			
D_{10}	2.0 ± 0.2	2.4 ± 0.2	2.9 ± 0.3
D_{25}	2.3 ± 0.2	2.9 ± 0.3	3.3 ± 0.3
D_{50}	2.5 ± 0.3	3.2 ± 0.3	4.7 ± 0.5
D_{75}	2.7 ± 0.3	4.8 ± 0.6	5.1 ± 0.5
D_{90}	5.8 ± 0.6	7.6 ± 0.8	9.7 ± 1.0
Uniformity of cell size distribution (μm)			
$D_{90}-D_{10}$	3.8 ± 0.4	5.2 ± 0.5	6.8 ± 0.7

Generally, the panels foamed with the dolomite foaming agent were with a more uniform cell-size distribution and lower average bubble size. The most uniform cell-size distribution was achieved in foam samples foamed with the minimum surface concentration ($2.5 \times 10^{-3} \text{ mg}/\text{mm}^2$) of dolomite powder, **Figure 3**.

The experimentally determined values of the average bubble radius in the foamed panels were at least for one

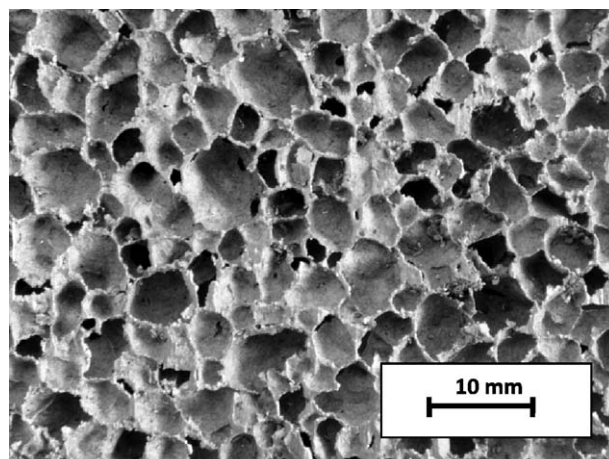


Figure 3: The homogeneous microstructure of the Al foam made from the ARB precursor with dolomite particles as the foaming agent. The ARB precursor was made by four roll-bonding cycles.

Slika 3: Homogena mikrostruktura vzorca Al-pene iz prekurzorja, izdelanega po postopku večstopenjskega topllega valjanja

order of magnitude higher than those predicted by the model. The reason for that difference is in effects limiting the stability of the individual bubbles, which are not considered by the model. These effects are as follows: bubble flow, drainage, rupture or coalescence, and coarsening.

From the difference between the theoretically predicted and experimentally determined values of the bubble radius, it is possible to estimate the stability of the real foam systems considered in this work. The experimental findings clearly confirm that coarser bubbles are more stable than finer ones. In addition, it is also evident that the stability of the bubbles is much higher in foams created by dolomite particles than in the counterparts foamed by TiH_2 . However, in both cases the average bubble sizes are proportional to the average initial size of the foaming particles – finer foaming particles lead to finer bubbles, while coarser ones lead to larger bubbles, as was predicted by the model.

On the other hand, the density of the aluminium foam samples was inversely proportioned to the bubble radius: the foam samples with finer bubbles had the higher density and, in contrast, the foam samples with larger bubbles were specifically lighter. At the same time and under the same foaming conditions (temperature, time), the foams made with the dolomite were with a significantly lower density than the samples with similar cell size foamed by the TiH_2 .

As is evident from the cell-size distribution data listed in **Tables 3 and 4**, an increase of the foaming-agent surface concentration (either TiH_2 or dolomite) leads to the formation of foams with larger bubbles and a lower density. However, also in that case, the samples foamed with dolomite were with smaller bubbles and lower densities.

The experimentally developed foam microstructures were mostly influenced by the degree of foam movement slowing down (i.e., the foam stability) attained in particular trials. In addition, the microstructure of foams was also influenced in some cases by the layered structure of the ARB precursors.

The slowing down of the movement of the foam includes the prevention of flow (the movement of bubbles with respect to each other caused either by external forces or changes in the internal gas pressure during foaming), drainage (flow of liquid metal through the foam), coalescence (sudden instability in a bubble wall leading to its disappearance) and coarsening (slow diffusion of gas from smaller bubbles to bigger ones).

The layered structure of the ARB precursors caused, in some samples, the appearance of so-called "line segregation", i.e., the flow of liquid metal across the line, **Figure 4**. Such segregation is most probably involved in the non-sufficient and/or different plastic deformation of individual layers during various roll-bonding cycles.

Generally, the foam stability in the liquid and semi-solid state of an aluminium alloy is improved by increasing the thickness of the bubble wall, decreasing the surface tension of the molten metal and increasing its viscosity. Simultaneously decreasing the surface tension and increasing the viscosity of molten aluminium can be achieved by introducing to the molten metal some amount of ceramic particles, e.g., formed in situ, by the thermal decomposition of the foaming agent at the interface between molten aluminium and the gas phase.

Quantitatively, the foam stability in the liquid and semi-solid state might be expressed by a dimensionless foam-stability factor (FSF), which we defined as:

$$FSF = X_0 \eta / (\sigma t) \quad (14)$$

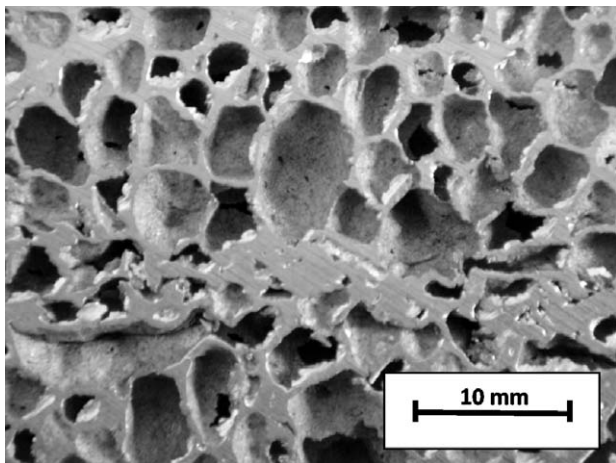


Figure 4: The characteristic "line segregation" in the samples of aluminium foams made from ARB precursors using dolomite as a foaming agent

Slika 4: Značilno "linijsko izcejanje" v vzorcih aluminijske pene z dolomitom kot sredstvom za penjenje. Vzorci pene so iz prekurzorjev, izdelanih po postopku večkratnega toplega valjanja

where X_0 is the average distance between neighbouring bubbles (which is proportional to the wall thickness), η is the dynamic viscosity of the slurry, σ is the surface tension at the interface molten or semi-solid aluminium-gas and t is the foaming time.

Evidently, a higher FSF means better foam stability. Unfortunately, in practice, it is not easy to determine the viscosity and the surface tension of the slurry of the molten aluminium alloy and the foaming agent particulates as well as the wall thickness of bubbles during their growth. Because of that, the usage of FSF is mostly limited to theoretical and, to some level, qualitative considerations.

The main differences between the TiH_2 and the dolomite foaming agent, which influences the foam microstructure development, are the following: (i) in the nature and reactivity of products of its thermal decomposition and (ii) the temperature interval of thermal decomposition.

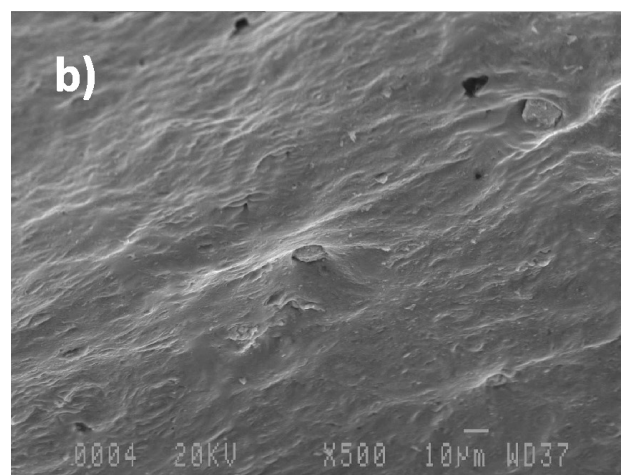
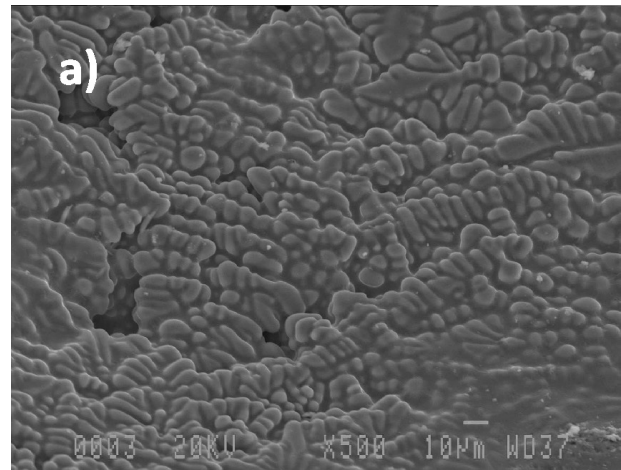
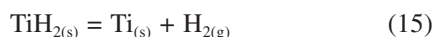


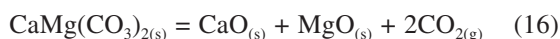
Figure 5: SEM micrograph of the internal surface of the bubble wall: a) bubble wall fully covered by Al_2O_3 , CaO and MgO particles in bubbles foamed by dolomite and b) clean internal surface in bubbles foamed by TiH_2

Slika 5: SEM-posnetek notranje površine por: a) nastale z razkrojem dolomita ter povsem prevlečene z delci Al_2O_3 , CaO in MgO in b) neprevlečene, nastale z razkrojem TiH_2

In ARB precursors with TiH_2 , the thermal decomposition of the foaming agent was observed starting from approximately $350\text{ }^\circ\text{C}$. The TiH_2 decomposes to $\text{Ti}_{(s)}$ and $\text{H}_{2(g)}$, Eq. 15, which do not tends to react with molten aluminium in the way of creating secondary ceramic phases making it possible to slow down the movement of the foam. Because of that, the internal surface of the bubble wall foamed by the TiH_2 is clean (**Figure 5b**).



In contrast to this, the thermal decomposition of the dolomite foaming agent, Eq. (16), proceeded above $700\text{ }^\circ\text{C}$, resulting in highly reactive products: $\text{MgO}_{(s)}$, $\text{CaO}_{(s)}$ and $\text{CO}_{2(g)}$ ⁷.



CaO and MgO are in the form of solid particulate aggregates, appearing at the molten metal- $\text{CO}_{2(g)}$ interface, while $\text{CO}_{2(g)}$ reacts with the molten aluminium in a bubble covering bubble internal surface with a thin, mostly continuous, film of Al_2O_3 (**Figure 5a**). Therefore, all the products of the dolomite thermal decomposition (MgO ,

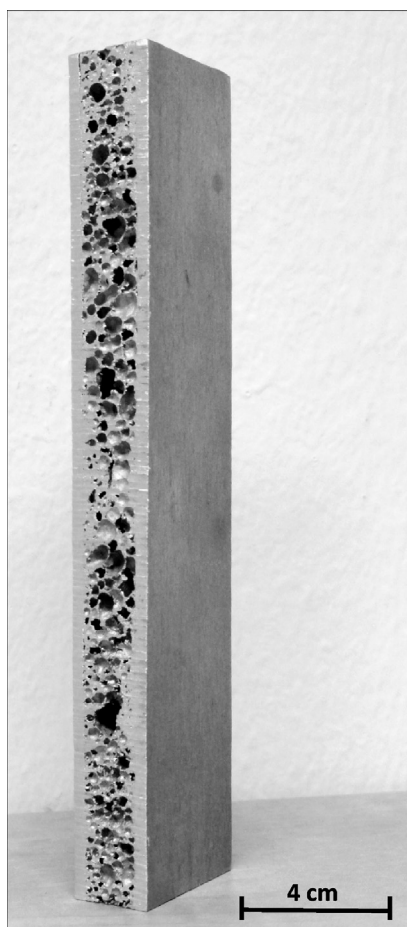


Figure 6: The cross-section of the prototype core-foamed panel made from ARB precursor with dolomite particles as the foaming agent.

Slika 6: Prečni prerez prototipnega panela s sredico iz aluminijске pene. Panel je izdelan iz večstopenjsko toplo valjanega prekurzorja z dolomitom kot sredstvom za penjenje

CaO and Al_2O_3) are very effective in slowing down the foam movement, decreasing the surface tension and increasing the local viscosity of the slurry. Due to the limited foam movement, bubbles in solidified samples remain significantly finer, resulting in foams with a higher density (a lower volume fraction of bubbles).

4.2 Fabrication of prototype core-foamed aluminium panels

Accumulative hot-roll bonded precursors with dolomite particles as a foaming agent were successfully foamed to core-foamed panels with a wall thickness of about 2 mm and a thickness of the foamed core of about 10 mm. The flat panel samples (approx. 150 mm long and 80 mm wide) were routinely foamed from the ARB precursors using the existing laboratory capabilities, **Figure 6**.

5 CONCLUSION

Our experimental findings confirmed that the ARB procedure is very promising (semi)-industrial route for the production of precursors for core-foamed aluminium panels. By combining a pair of AA1050 aluminium alloy strips and various foaming agents (TiH_2 or dolomite powders), several foaming precursors were prepared through two to four cycles of ARB and successfully foamed into core-foamed aluminium panels.

The use of dolomite powder as a foaming agent with a higher temperature of thermal decomposition ($>700\text{ }^\circ\text{C}$) compared to TiH_2 , which thermally decomposed even at the temperature of hot-rolling ($>350\text{ }^\circ\text{C}$), enabled the formation of multilayered precursors at higher temperatures of the hot-rolling without any intermediate annealing. This significantly improved the productivity of the production of core-foamed aluminium panels without influencing their final quality.

The microstructure uniformity and stability of the foams made from ARB precursors depend on the surface concentration and morphology of the foaming agent as well as on the foaming temperature.

Acknowledgement

This work was supported by funding from the Public Agency for Research and Development of the Republic of Slovenia, as well as the Impol Aluminium Company and Bistral, d. o. o., from Slovenska Bistrica under contract No. 2410-0206-09.

6 REFERENCES

- ¹ N. Tsuji, Y. Saito, S. H. Lee, Y. Minamino, *Adv. Eng. Mater.*, 5 (2003) 5, 338
- ² Y. Saito, H. Utsumonia, N. Tsuji, T. Sakai, *Acta Mater.*, 47 (1999), 579
- ³ K. Kitazono, E. Sato, K. Kuribayashi, *Scripta Mater.*, 50 (2004), 495

- ⁴ K. Kitazono, E. Sato, *Materials Science Forum*, 475–479 (2005), 433
- ⁵ L. E. G. Cambonero, J. M. R. Roman, F. A. Corpas, J. M. R. Prieto, *Journal of Materials Processing Technology*, 209 (2009), 1803
- ⁶ D. P. Papadopoulos, H. Omar, F. Stergioudi, S. A. Tsipas, N. Michailidis, *Colloidal and Surfaces A: Physiochem. Eng. Aspects*, 382 (2011), 118
- ⁷ V. Gergely, D. C. Curran, T. W. Clyne, *Composites Science and Technology*, 63 (2003), 2301
- ⁸ V. Kevorkijan, S. D. Škapin, I. Paulin, B. Šuštaršič, M. Jenko, *Mater. Tehnol.*, 44 (2010) 6, 363
- ⁹ US Pat. No. 7.452.402 issued on November 18, 2008